Effect of VN buffer layer on the magnetic anisotropy of epitaxial $Ni_{80}Fe_{20}$ thin films deposited on MgO (001) substrates

M. T. Sultan*, A. Tryggvason*, U. B. Arnalds*, S. Ingvarsson
*Science Institute, University of Iceland, Reykjavík, Iceland
Email: muhammad@hi.is

***Abstract*—This study incorporates the structural and magnetic characterization of epitaxial $Ni_{80}Fe_{20}$ films grown by direct current magnetron sputtering on MgO(001) and MgO(001)||VN(001) substrates. A series of samples grown with different N_2 flow settings for the deposition of VN and similar permalloy deposition parameters was utilized to investigate the effect of morphological evolution and buffer layer induced strain on the magnetic properties of $Ni_{80}Fe_{20}$. X-ray diffraction analysis reveals an epitaxial nature of the VN(001) and Py(001) films grown on MgO substrates. Angular dependent magneto-optical Kerr effect characterization reveals a cubic anisotropy for $Ni_{80}Fe_{20}$ on MgO with a coercivity of ∼0.8 Gauss along the easy directions. Incorporating an epitaxial VN buffer, the structures showed a transition from a cubic to isotropic magneto-crystalline anisotropy with coercivity varying from 2.5 to 25 Gauss for $Ni_{80}Fe_{20}$ deposition on VN (with N_2 varying from 5 to 12 sccm). The variation is attributed to the microstructural evolution of the $Ni_{80}Fe_{20}$ to 3D structures along with an induced structural strain.**

***Index Terms*—$Ni_{80}Fe_{20}$, VN, MgO, strain, magnetic anisotropy, MOKE**

I. Introduction

Permalloy ($Ni_{80}Fe_{20}$, denoted as Py) is a widely recognized material for its application in telecommunications, sensors, magnetic storage and magnetic random access memory [1]–[3]. Among other things, this is due to its small magnetocrystalline anisotropy and magnetostriction, low coercivity and high permeability [1], [4]. In this context films with a uniaxial anisotropy are preferred in magnetic devices as they provide easier control of the magnetization direction of devices. However, biaxial magnetic anisotropy has recently been recognized to be advantageous compared to systems showing uniaxial anisotropy [5].

Epitaxial Py grown by various methods tends to display a perfect lattice, while the arrangements of the Ni and Fe may be disordered to varying degree [4]. Permalloy films can be grown in epitaxial single crystal form, polycrystalline, often with (111) texture and/or sometimes with a nanostructured film surface [1], [4], [6]–[9]. Moreover, the relative magnitude and strength of magnetic anisotropy between the uniaxial and cubic anisotropy of permalloy films, and ferromagnetic thin films in general, depends on material parameters such as film thickness, substrate type and roughness, buffer layer, interface and the strain condition [1], [5], [10]–[13]. In this work we present the structural and magnetic properties of epitaxial permalloy on MgO and MgO/VN. Our work highlights the correlation between strain, induced by the underlying epitaxial-VN buffer layer, (grown under varying N_2 flow settings) and the resulting surface morphology on the magnetic properties of Py.

II. Materials and methods

The Py thin films (thickness ∼50 nm) were deposited on to MgO (001) substrates with and without the application of a VN buffer layer. Table 1 summarizes the structure of our samples. Films of VN were synthesized by reactive direct current magnetron sputtering (r-dcMS) from a vanadium target at a constant power of 200 W using a custom-built sputter chamber [14]. Prior to deposition the chamber was held at a base pressure of 8×10^{-9} mbar, and the substrates were pre-baked at 600°C for 30 minutes. For sputtering we used Ar as the working gas along with N_2 as the reactive gas and a throttle valve was adjusted to stabilize the growth pressure to 7×10^{-3} mbar. The flow rates $q_{\mathrm{Ar}} = 40$ sccm and $q_{\mathrm{N_2}} = 5$ - 12 sccm, were set using mass flow controllers. During VN deposition, the substrates were held at 600°C. After which the films were cooled down *in-situ* under vacuum up to 400°C. The Py films of ∼ 50 nm were then deposited by dcMS using $Fe_{20}Ni_{80}$ target at a constant power of 80 W and at a growth temperature of 400°C and growth pressure of 7×10^{-3} mbar.

TABLE I
Overview of deposited structure along with respective film thickness.

Sample Id.	***VN*** (nm)	***N*** (sccm)	***Py*** (nm)	***Structure***
Py	-	-	50	MgO/Py
VNP1	50	5	50	MgO/VN/Py
VNP2	50	8	50	MgO/VN/Py
VNP3	50	12	50	MgO/VN/Py

X-ray reflectivity (XRR) and x-ray diffraction (XRD) measurements along with pole scans were performed using a Panalytical X'pert diffractometer (CuKα, 0.15406 nm). A detailed description of our x-ray diffraction analysis is provided in our previous works [4], [15]. An atomic force microscope (AFM), from Park System (PSIA XE-100) was utilized for surface analysis. In-plane magnetic anisotropy analysis was carried out using a custom built longitudinal magneto-optical Kerr effect (MOKE) setup to measure magnetic hysteresis as a function of the azimuth angle [16].

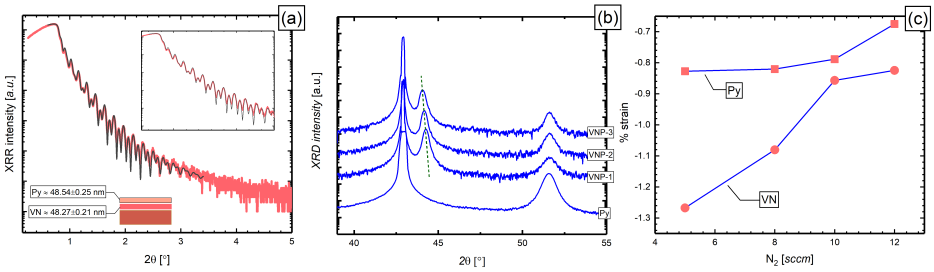

Fig. 1. (a) XRR plot for Py on MgO/VN along with simulated data (red line). (b) XRD plots for Py on MgO and Py on MgO/VN where the VN layer was deposited with different N_2 flow settings. Legends refer to Table 1 for structural details. (c) Percentile strain extracted using (002) peaks in (b) and corresponding d-spacing and a-lattice parameter for VN and Py films.

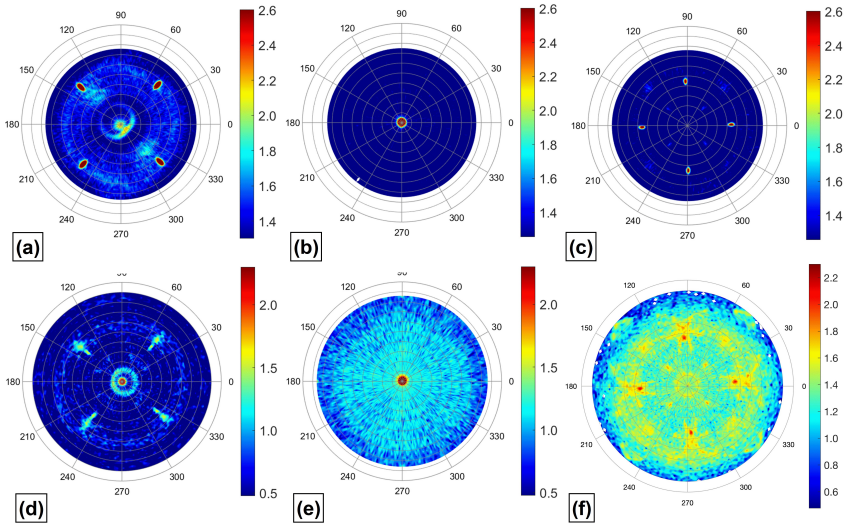

Fig. 2. Pole scans along (111), (200) and (220) planes for structures (a-c)Py and (d-f) VNP-3, respectively. The respective colour bars represent normalized log intensity in arbitrary units.

III. Results and Discussion

A. Structural characterization

The thickness and roughness of films were determined using XRR scans. A typical XRR scan performed on the MgO/VN/Py structure is shown in Fig. 1(a), along with simulated data, utilized to determine the films thickness Fig. 1(b) shows the X-ray diffraction plots for respective structures. The XRD scans reveal a high intensity peak attributed to MgO at $2\theta = 42.971°$. They also show an epitaxial Py (100) peak located at $\sim 51.5°$. For Py on MgO the results indicate an orientation relationship of MgO[100]||Py [100]. For Py films on MgO/VN (where VN is deposited at varied N_2 settings) the XRD reveals an epitaxial relation of the VN and Py layers. However, by increasing N_2 flow an evident shift in VN peak position is observed towards lower angles implying relaxation of the VN in the out-of-plane direction. The strain estimated via (002) peaks for both VN and Py is plotted in Fig. 1(c).

Fig. 2 shows the pole scans for structures deposited at 400°C on the (001) MgO and MgO/VN substrates. For each respective structure the pole scan around the (200) plane reveal an intense peak at $\psi = 0°$ complementing the epitaxial relation of the Py film on the MgO(001) substrate, i.e. with the (002) plane lying parallel to the substrate. The (220) and (111) pole scans show a four fold symmetry. For the pole scan around (111) the spots at $\phi = 45°$ and $\psi = 54.74°$ are obtained as expected from the angle between (002) and 111 planes. Whereas, the pole scan around (220) showed four fold spots at ψ 45° and 90° , in good agreement with the symmetry in a cubic single crystal of the film [4].

Fig. 3 shows the surface morphology of all samples investigated by atomic force microscopy and will be discussed later in later section. The measurements were repeated on different reference areas to validate the reproducibility of observed features. An obvious presence of 3D-nanostructures can be observed, which for Py on MgO/VN increase in size with increase in nitrogen content. The roughness (R_q) values estimated are $\sim$ 1.7, 1.2 and 4.5 nm for structure in Fig. 3(a-c), respectively.

B. Magnetic properties

Fig. 4 shows the coercivity and relative magnetic remanence (M_{rem}/M_{sat}) extracted from hysteresis loops measured for in-plane sample angles using MOKE with an in-plane applied

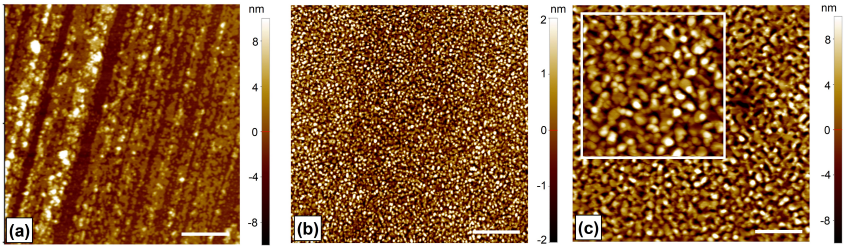

Fig. 3. 5×5 μm^2 AFM micrographs of structures labelled (a) Py, (b) VNP1 and (c) VNP3. The scale bar provided in the figures are 1μm.

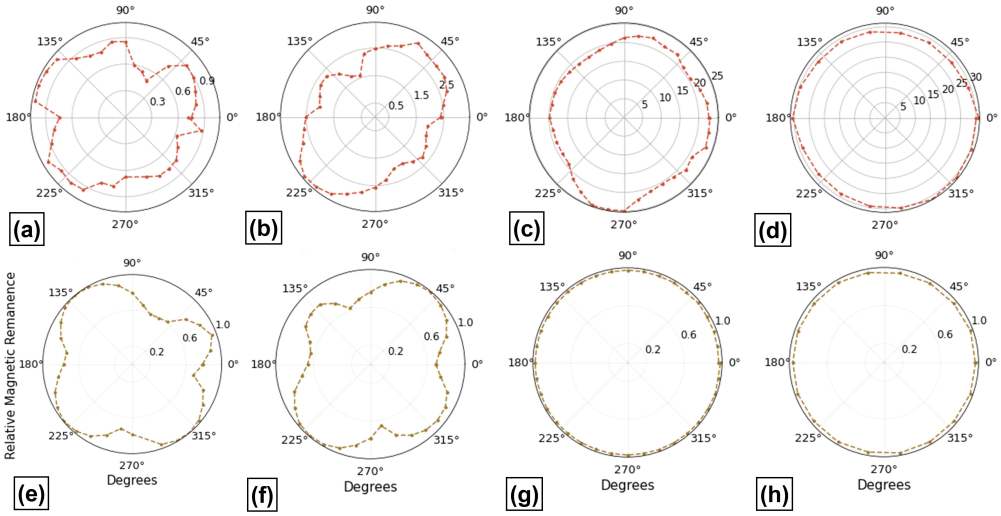

Fig. 4. In-plane polar plots for (a-d) coercivity in Oersteds (note the different scales) and (e-h) M_{rem}/M_{sat} for Py, VNP1, VNP2 and VNP3 structures, respectively. The values were extracted from hysteresis loops recorded for varying in-plane sample angles ($0^\circ - 360^\circ$) in the MOKE setup.

magnetic field. The polar plots obtained for structures reveal that the $Ni_{80}Fe_{20}$ films on MgO (see Fig. 4(a, e)) and on VN/MgO (VNP1, see Fig. 4(b, f)) display a soft magnetic behavior with coercivity of $\sim$0.8 Gauss and 2.5 Gauss, respectively, along easy axes. The samples display a four-fold magnetocrystalline anisotropy with easy axes along $\sim$140° (315°) and 45° (225°). However, with increase in N_2 flow setting from 5 to 12 sccm for VN deposition (i.e. VNP2 - VNP3, Fig. 4(c, g and d, h)), the polar plots for coercive field and M_{rem}/M_{sat} hysteresis loops showed increasingly isotropic characteristics. The observed change in magnetocrystalline anisotropy feature from cubic to isotropic can be attributed to strain and the microstructural evolution as discussed in references [1], [13], [17].

It is apparent from our data that induced strain strongly affects the magnetic anisotropy of the Py films. This is in line with the findings of Cao *et al.* [13] in FeGa films on Cu substrates, where they observed that with reduction in the out-of-plane compressive strain the magnetocrystalline anisotropy tends to show a transition from uniaxial anisotropy towards an isotropic nature. However, with the still outspread belief that Py has almost zero magnetostriction, this may come as a surprise. This need not be, as it is well established that in *ultrathin film* form Py exhibits strong magnetostrictive response [1], [4], [18]. As shown theoretically for Py on MgO under compressive strain in the out-of-plane direction [1], an increase in our N_2 flow settings along with a reduction in the out-of-plane compressive strain (Fig. 1(c)), causes a transition from cubic to isotropic nature of the magnetocrystalline anisotropy. Furthermore, the pole scans along the (111) and (220) planes are radically elongated along the ψ axis especially for Py on MgO/VN. This implies that the lattice constants are expanded in-plane which is in good agreement with the shift in peak position towards lower angles i.e., a reduction in out-of-plane compressive strain [4].

The observed variation in magnetocrystalline anisotropy from cubic to an isotropic nature is supported by work by Michelini *et al.* [1]. They showed that for epitaxial Py on MgO the morphology of the Py films changes from flat to a 3D nanostructure formation with increase in growth temperature from 300 to 500°C, thereby resulting in a transition from uniaxial anisotropy to a four-fold magnetocrystalline anisotropy. These results are in good agreement with our analysis (see Fig. 5) showing M_{rem}/M_{sat} for Py on MgO deposited at RT and at 400°C). This effect of the morphological evolution on the anisotropy is in good agreement with microstructural

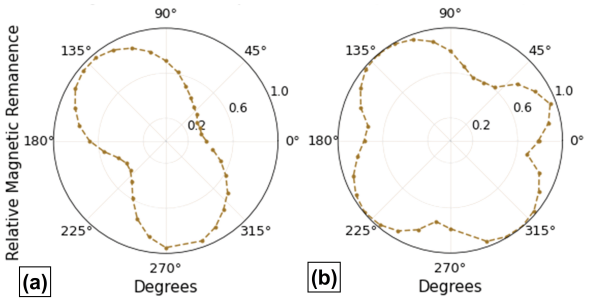

Fig. 5. In-plane polar plots for M_{rem}/M_{sat} for Py deposited at (a) room temperature and (b) 400°C. The values were extracted from hysteresis loops recorded for varying in-plane sample angles (0° - 360°) in a MOKE setup.

evolution evident in our AFM results (cf. Fig. 3, revealing the formation of 3D nanostructures). For Py on MgO/VN it can be seen that with increase in N content, and consequent reduction in compressive strain, the grain size increases to compensate for strain relaxation [15]. This results in the initial cubic anisotropy evolving into isotropic behavior.

From the above analysis it can be understood that the competing factors i.e., from the substrate, nitrogen stoichiometry, crystallinity, surface morphology, film and buffer layer thickness (not discussed here) determine the strain in structures which in turn affects the magnetic properties of the films.

IV. Conclusions

In summary we investigate the effect of structural and morphological evolution with corresponding strain on the magnetocrystalline anisotropy of epitaxial Py on MgO and MgO/VN. The epitaxial nature of $Ni_{80}Fe_{20}$ films was confirmed by XRD and pole scans along (200), (111) and (220) planes. For $Ni_{80}Fe_{20}$ film on MgO with VN buffer layer it was observed that for increasing N content the variation in induced interficial strain and surface layer morphology plays a vital role in determining the magnetocrystalline anisotropy. That is with reduced out-of plane compressive strain and increased size of 3D nanostructures, the structure showed transition from cubic to isotropic nature. Furthermore, the four-fold anisotropy observed in $Ni_{80}Fe_{20}$ films deposited at 400°C is attributed to a microstructural evolution from 2D layer growth to 3D nanostructure formation and is validated by its comparison with structures having $Ni_{80}Fe_{20}$ deposited at room temperature exhibiting uniaxial anisotropy along [100] direction.

Acknowledgment

This work was supported by funding from the Icelandic Research Fund Grant Nos. 218029-051, 228951-051 and 207111-051.

References

[1] F. Michelini *et al.*, "Permalloy thin films on MgO(001): Epitaxial growth and physical properties," *Journal of Applied Physics*, vol. 92, pp. 7337–7340, dec 2002.

[2] T. Ohtani *et al.*, "Magnetostriction of permalloy epitaxial and polycrystalline thin films," *EPJWC*, vol. 40, p. 11004, 2013.

[3] A. A. Chlenova *et al.*, "Permalloy-Based Thin Film Structures: Magnetic Properties and the Giant Magnetoimpedance Effect in the Temperature Range Important for Biomedical Applications," *Sensors 2017, Vol. 17, Page 1900*, vol. 17, p. 1900, aug 2017.

[4] M. Kateb, J. T. Gudmundsson, and S. Ingvarsson, "Effect of atomic ordering on the magnetic anisotropy of single crystal $Ni_{80}Fe_{20}$," *AIP Advances*, vol. 9, mar 2019.

[5] Y. Jeong *et al.*, "Buffer layer dependence of magnetic anisotropy in Fe films grown GaAs substrate," *Solid State Communications*, vol. 200, pp. 1–4, dec 2014.

[6] M. Kateb and S. Ingvarsson, "Correlation of uniaxial magnetic anisotropy axes and principal resistivities in polycrystalline ferromagnetic films," *Journal of Magnetism and Magnetic Materials*, vol. 532, p. 167982, 2021.

[7] C. Blaas, L. Szunyogh, P. Weinberger, C. Sommers, and P. M. Levy, "Electrical transport properties of bulk ni_cfe_{1-c} alloys and related spin-valve systems," *Physical Review B*, vol. 63, no. 22, p. 224408, 2001.

[8] M. Ishino, J. Yang, K. Makihara, J. Shi, and M. Hashimoto, "Epitaxial growth and physical properties of Permalloy film deposited on MgO(001) by biased dc plasma sputtering," *Journal of Vacuum Science & Technology A: Vacuum, Surfaces, and Films*, vol. 18, p. 2339, sep 2000.

[9] M. Kateb, H. Hajihoseini, J. T. Gudmundsson, and S. Ingvarsson, "Role of ionization fraction on the surface roughness, density, and interface mixing of the films deposited by thermal evaporation, dc magnetron sputtering, and HiPIMS: An atomistic simulation," *Journal of Vacuum Science & Technology A*, vol. 37, no. 3, p. 031306, 2019-05.

[10] A. Stupakiewicz *et al.*, "Interface magnetic and optical anisotropy of ultrathin Co films grown on a vicinal Si substrate," *Physical Review B - Condensed Matter and Materials Physics*, vol. 80, p. 094423, sep 2009.

[11] S. V. Komogortsev *et al.*, "Advanced Characterization of FeNi-Based Films for the Development of Magnetic Field Sensors with Tailored Functional Parameters," *Sensors 2022, Vol. 22, Page 3324*, vol. 22, p. 3324, apr 2022.

[12] S. Wang, T. Gao, C. Wang, and J. He, "Studies of anisotropic magnetoresistance and magnetic property of $Ni_{81}Fe_{19}$ ultra-thin films with the lower base vacuum," *Journal of Alloys and Compounds*, vol. 554, pp. 405–407, mar 2013.

[13] D. Cao *et al.*, "Controllable magnetic and magnetostrictive properties of FeGa films electrodeposited on curvature substrates," *Applied Physics A: Materials Science and Processing*, vol. 122, pp. 1–6, nov 2016.

[14] U. B. Arnalds *et al.*, "A magnetron sputtering system for the preparation of patterned thin films and in situ thin film electrical resistance measurements," *Review of Scientific Instruments*, vol. 78, p. 103901, oct 2007.

[15] M. Sultan, K. Ignatova, E. Thorsteinsson, and U. Arnalds, "Structural morphology and electrical transitions of v_2o_3 thin films grown on sio_2/si by high power impulse magnetron sputtering," *Thin Solid Films*, vol. 742, p. 139048, 2022.

[16] K. A. Thórarinsdóttir, N. Strandqvist, V. V. Sigurjónsdóttir, E. B. Thorsteinsson, B. Hjörvarsson, and F. Magnus, "Finding order in disorder: Magnetic coupling distributions and competing anisotropies in an amorphous metal alloy," *APL Materials*, vol. 10, p. 041103, apr 2022.

[17] S. S. Ahmad *et al.*, "Effect of Cu buffer layer on magnetic anisotropy of cobalt thin films deposited on MgO(001) substrate," *AIP Advances*, vol. 6, p. 115101, nov 2016.

[18] O. Song, C. A. Ballentine, and R. C. O'Handley, "Giant surface magnetostriction in polycrystalline Ni and NiFe films," *Applied Physics Letters*, vol. 64, pp. 2593 – 2595, 05 1994.